pubs.acs.org/Biomac

Article

Molecular Design of Lignin-Derived Side-Chain Phenolic Polymers toward Functional Radical Scavenging Materials with Antioxidant and Antistatic Properties

Maarten Rubens,* Panagiotis Falireas, Karolien Vanbroekhoven, Wouter Van Hecke, Görkem Eylül Kaya, Bilge Baytekin, and Richard Vendamme

Cite This: *Biomacromolecules* 2023, 24, 3498−3509

Read Online

ACCESS | Metrics & More | Article Recommendations | Supporting Information

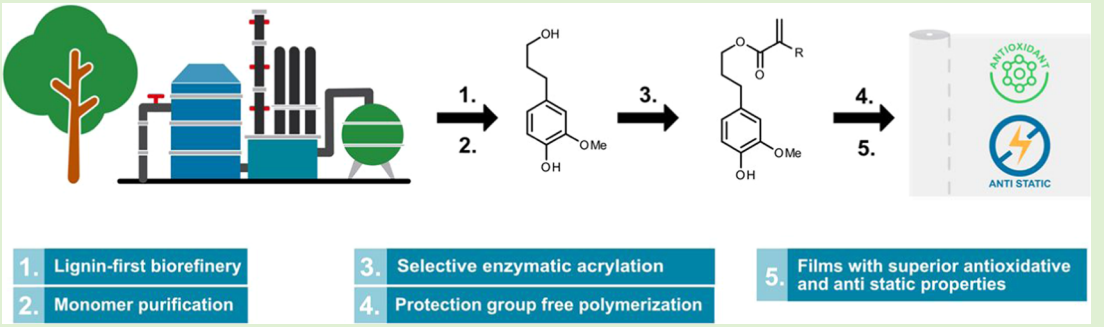

ABSTRACT: This article reports a new family of functional side-chain phenolic polymers derived from lignin monomers, displaying a combination of properties that are usually mutually exclusive within a single material. This includes a well-defined molecular structure, transparency, antioxidant activity, and antistatic properties. Our design strategy is based on the lignin-derived bioaromatic monomer dihydroconiferyl alcohol (DCA), a promising and yet largely unexplored asymmetrical diol bearing one aliphatic and one phenolic hydroxyl group. A lipase-catalyzed (meth)acrylation protocol was developed to selectively functionalize the aliphatic hydroxy group of DCA while preserving its phenolic group responsible for its radical scavenging properties. The resulting mono-(meth)acrylated monomers were then directly copolymerized using reversible addition-fragmentation chain-transfer (RAFT) polymerization without any protection of the phenolic side chains. Kinetics studies revealed that, under select conditions, these unprotected phenolic groups surprisingly did not inhibit the radical polymerization and lead to polymers with defined molar masses, low dispersities, and block copolymers. Finally, applications of these new radical scavenging polymers were demonstrated using an antioxidant assay and antistatic experiments. This research opens the door to the direct incorporation of natural antioxidants within the synthetic polymer backbones, increasing the biobased content and limiting the leaching of potentially harmful additives.

INTRODUCTION

Lubricants, fuels, plastics, and all organic matter are prone to oxidation.[1,2] The generation of peroxyl radicals causes this oxidative degradation. Antioxidants, as the name indicates, are compounds that delay or inhibit this oxidative process.[3] These preserving additives are of paramount importance in pharmaceuticals, food and beverages, lubricants, and polymer chemistry. Although there are many known natural antioxidants, the most used antioxidants are synthetic, petrol-derived compounds such as butylated hydroxytoluene (BHT), butylated hydroxyanisole (BHA), and *tert*-butyl hydroquinone (TBHQ).[4] Despite their strength, these molecules are known to migrate from their polymer matrix into the packaged material or environment, which is highly undesirable.[5]

Hindered phenols have been one of the most used compounds as antioxidants since the 1920s.[1] Lignin, being a natural polyphenolic structure, is the ideal candidate for serving as a renewable, nontoxic antioxidant.[6] In addition to its antioxidant character, it has also been recently demonstrated that the radical scavenging capacity of lignin makes it possible to elucidate the antistatic nature of wood.[7] Lignin is the second most abundant biopolymer by weight, only being surpassed by cellulose, and represents the largest source of natural aromatics, which are crucial building blocks in the chemical industry.[8] Unfortunately, lignin is still not being valorized effectively. To this date, lignin is considered a byproduct of the pulp-and-paper industry, whereby the harsh chemical con-

Received: March 17, 2023
Revised: May 2, 2023
Published: May 11, 2023

https://doi.org/10.1021/acs.biomac.3c00275
Biomacromolecules 2023, 24, 3498−3509

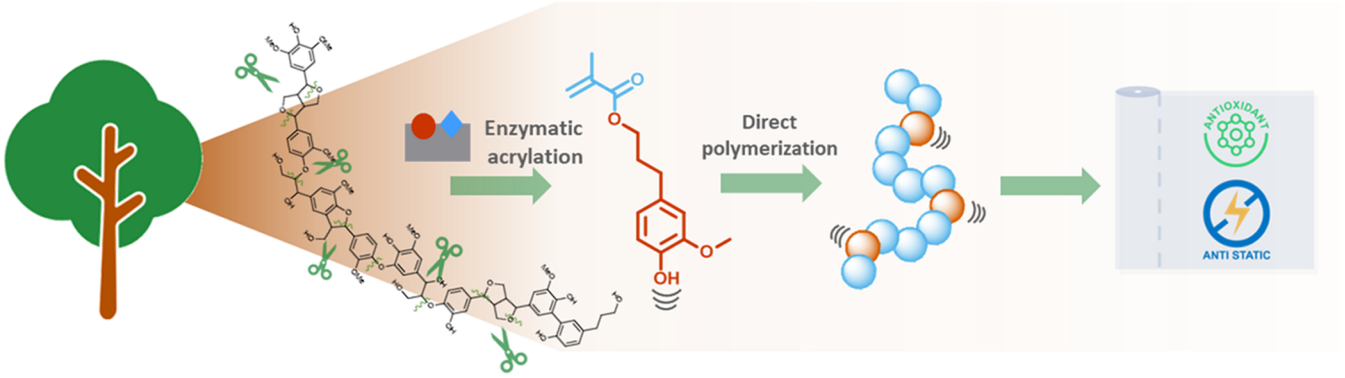

Figure 1. Conceptual overview of the current work. Lignin-derived acrylic polymers with outstanding antioxidative properties by the selective lipase-catalyzed (meth)acrylation of the DCA (synthetic) and its subsequent direct RAFT copolymerization into thermoplastic poly(meth)-acrylates.

ditions used in cellulose extractions result in a heterogeneous recalcitrant lignin that is hard to valorize. To that end, multiple millions of tons of lignin are only utilized as a low-cost fuel for power and heat generation while holding a vast potential as a reliable and renewable feedstock for chemicals and materials.[9]

To further circumvent these drawbacks, lignin depolymerization has emerged as a promising mitigation strategy.[10] Depolymerization of pristine lignin back to its monolignol building blocks (via the cleavage of the β-O-4 while avoiding repolymerization) results in lignin fractions of low molecular weight and depending on the exact process used in true bio-oils, which are rich in monomers (up to 50 wt %), dimers, and oligomers.[11] These so-called lignin bio-oils have improved properties in terms of functionality, solubility, and reactivity and are nowadays successfully valorized as starting material for epoxides and polyurethanes.[12] The most prevalent monomers found in depolymerized lignin are monolignols such as propyl guaiacol (PG), propyl syringol (PS), dihydroconiferyl alcohol (DCA), and dihydrosinapyl alcohol (DSA), and the ratio of them in the bio-oil depends on the choice of feedstock, catalyst, and process conditions. Fractionation and distillation are common strategies to separate these monomers with high purity.[13]

Until now, the exploitation of lignin's antioxidant and antistatic activities in polymer chemistry has been limited to using it as an additive in thermoplastic polymers, with only a few examples of thermosets containing lignin that have been assessed for their antioxidant activity.[14] In contrast, the covalent incorporation of discrete lignin-derived monomers into a polymer matrix to add antioxidant and antistatic activities has remained unexplored. This would ensure that the leaching of potentially harmful additives from the polymer matrix into its surroundings does not occur while at the same time providing a natural alternative for the commercially used fossil-derived antioxidants such as BHT, BHA, and TBHQ.

Recently, the group of Epps elegantly has shown how lignin-derived acrylic monomers can be incorporated into polymers.[15−17] Monofunctional lignin-derived dimethoxy phenol was chemically (meth)acrylated by reacting with the phenolic hydroxyl group and subsequently homopolymerized by free-radical polymerization. The resulting thermoplastic poly(dimethoxy phenyl methacrylate) polymers and statistical copolymers showed a wide T_g range, from less than 100 °C to greater than 200 °C.[16,18] Furthermore, all poly(dimethoxy phenyl methacrylate) (co)polymers exhibited thermal stability up to 300 °C in air and showed excellent solvent resistance. This highlights that lignin-derived acrylic monomers allow for tuning the polymer properties depending on the specific monomers used and that superior material properties over fossil-derived acrylics can be obtained, but unfortunately, with a loss of radical scavenging ability due to the functionalization of the phenolic hydroxyl group. Reversible addition-fragmentation chain-transfer (RAFT) polymerization of lignin-derived monomers allows for more complex polymers such as triblock copolymers to be made, which are utilized as pressure-sensitive adhesives.[19] Lignin oils rich in monomers were also methacrylated. By tuning the level of methacrylation and employing RAFT agents to control the molecular weight buildup, thermoplastic lignin-derived poly(methacrylate) was obtained from lignin oil without monomer purification and isolation.[20] Furthermore, it has been shown that this lignin-oil-derived acrylic resin can be applied in advanced manufacturing techniques such as three-dimensional (3D) printing by stereolithography.[21]

Functionalization of the lignin-sourced monomers with (meth)acrylate groups is exclusively performed by highly reactive and toxic chemical reagents such as (meth)acryloyl chloride and (meth)acrylic anhydride.[22] Moreover, these changes require the use of organic solvents, bases, or acids as catalysts and elaborate purification methods as toxic side products are formed. Also, using chemical methods does not permit the selective acrylation of the aliphatic hydroxyl groups over the aromatic hydroxyl group, with a loss of antioxidative properties as a result.

To this end, we developed a two-step process utilizing the lignin-derived monomer DCA and several green chemistry principles[23] (avoiding toxic reagents, solvent-free, low-temperature, and enzymatically catalyzed) for the direct synthesis of acrylic copolymers with antioxidative properties. First, (meth)-acrylated DCA was synthesized in neat conditions by the lipase-catalyzed selective (meth)acrylation of the aliphatic hydroxyl group.[24,25] This enzymatic strategy ensures that the phenolic hydroxyl groups stay intact. In contrast, a chemical acrylation would lead to preferential acrylation of the phenolic hydroxyl group over the aliphatic hydroxyl group due to its higher reactivity, leading to the loss of the required antioxidative properties. In a second step, the obtained monomers were copolymerized with 2-hydroxyethyl methacrylate (HEMA) and 4-hydroxybutyl acrylate (HBA) using thermal RAFT polymerization, which typically yields targeted

https://doi.org/10.1021/acs.biomac.3c00275
Biomacromolecules 2023, 24, 3498−3509

molecular weights, narrow dispersities, and copolymer composition control through the feed monomer molar ratios (Figure 1).

Typically, a protection−deprotection strategy of the phenolic hydroxyl group is required for the radical polymerization of phenolic monomers as they would quench the radicals required for the polymerization.[26] However, we showed that the radical RAFT polymerization can proceed uninhibited, despite large stoichiometric excess of the radical scavenging DCA (meth)acrylate monomers, under sufficient oxygen-free conditions. The RAFT copolymerization using DCA (meth)acrylate followed the kinetics typically observed in controlled radical polymerization and produced copolymers with narrow and targeted molar mass distributions. Furthermore, block copolymers were readily synthesized, further proving that irreversible quenching of the living end groups is avoided. The radical scavenging ability of hindered phenols acts through peroxyl radicals, which are formed by the reaction of a carbon-centered radical with oxygen.[27] We hypothesized that the irreversible termination could be prevented if the oxygen content is minimized, as this would eliminate the main inhibition pathway. Finally, the radical scavenging ability of the copolymers with various chain lengths and amounts of the active DCA (meth)acrylate monomer is measured through their antioxidative and antistatic properties.

EXPERIMENTAL SECTION

Materials. 4-Hydroxybutyl acrylate (HBA) was kindly provided by BASF (Ludwigshafen, Germany). The rest of the products were purchased from commercial sources: eugenol (Sigma-Aldrich, 99+%); borane dimethylsulfide complex (Alfa Aesar); hydrogen peroxide (Fisher BioReagents, 30 wt % in water); hydrochloric acid (Fisher Chemical, 37 wt %); sodium hydroxide (Acros Organics, >99.9%); magnesium sulfate (Acros Organics, 97%); methanol (MeOH, Fisher Chemical, 99.9%, degassed with N_2 prior to use in the DPPH test); tetrahydrofuran (THF, Acros Organics, 99+%, dried using molecular sieves (3 Å)); petroleum ether (40−60 °C boiling point range, Acros Organics 99+%); dichloromethane (DCM, Acros Organics, 99.6%); diethyl ether (Fisher Chemical, >99%); dimethyl formamide (DMF, Acros Organics, 99+%); 2,2-diphenyl-1-(2,4,6-trinitrophenyl)-hydrazinyl (DPPH, Cayman Chemicals ≥95,0%); 3,5-di-*tert*-butylhydroxytoluene (BHT, Supelco, ≥95,0%); methyl methacrylate (MMA, Alfa Aesar, 99%); methyl acrylate (MA, Alfa Aesar, 99%); 3,5-di-*tert*-butyl-4-hydroxyphenylpropionic acid (Alfa Aesar, 98%); hydroxyethyl methacrylate (HEMA, Alfa Aesar, 97%); 4-methoxyphenol (MEHQ, Sigma-Aldrich, 99%); phenothiazine (Sigma-Aldrich, 98%); Novozym 435 (Sigma-Aldrich); molecular sieves 5 Å (Sigma-Aldrich); aluminum oxide (activated, basic, Brockmann I, Sigma-Aldrich); hydroquinone (Sigma-Aldrich 99+%); azobisisobutyronitrile (AIBN, Sigma-Aldrich, 98%); and 2-cyano-2-propyl dodecyl trithiocarbonate (CDP-TTC, Sigma-Aldrich, 97%).

Analytical Techniques. Proton nuclear magnetic resonance spectroscopy (^{1}H NMR) was performed using a 400 MHz Bruker spectrometer or on a Magritek Spinsolve 80 Phosphor Benchtop NMR spectrometer. Chemical shifts are reported in ppm relative to solvent signal (DMSO or chloroform: δH = 2.50 ppm or δH = 7.26 ppm). The spectra were recorded at a temperature of 25 °C with the one-dimensional (1D) proton standard protocol using 16 scans with a 90° excitation pulse (7 μs); data processing was performed with MestReNova version 14.1.0 including zeroth- and first-order phase correction and baseline correction with a Bernstein polynomial fit of the third order.

Gel permeation chromatography (GPC) was performed on a Shimadzu system using a combination of three Styragel HRE4 columns connected to an RI and UV detector. The instrument was calibrated with polystyrene (PS) internal standards (162−204,000 g·mol^{-1}) and eluted with THF. Universal calibration and the Mark−Houwink parameters of HEMA (K = 2.39 10^{-4} dL·g^{-1}, α = 0.537) and a dn/dc = 0.056 mL·g^{-1}[28] were used for the molar mass determination of the DCAMA-HEMA copolymers. For the copolymers of DCAA-HBA, PS equivalents were used to calculate the molar mass.

Liquid chromatography−mass spectrometry (LC−MS) was performed on a Thermo Vanquish coupled to a Thermo Q Exactive using electrospray ionization (ESI) in positive and negative ion modes with a scan range from 100 to 1500 m/z. An Acquity BEH C18 100 mm × 2.1 mm, 1.7 μm column was used. A solvent gradient of 0 min: 5%B, 2 min: 5%B, 20 min: 100%B, 25 min: 100%B. 25.5 min: 5%B, 30 min: 5%B was used at 60 °C, and the absorption spectra were measured between 190 and 680 nm. Solvent A consists of 10 mM NH_4Ac in Milli-Q water and solvent B is a mixture of 70 v/v% acetonitrile and 30 v/v% isopropanol.

The antioxidant activity was determined by the free-radical scavenging activity test using DPPH, as reported in the literature.[29] A 30 μg/mL stock solution of DPPH was prepared in methanol and was stored in the dark under a nitrogen atmosphere at 4 °C. A calibration curve was obtained by measuring the UV absorbance of DPPH solutions in methanol at a concentration range from 5 to 200 μg/mL. Stock solutions of 1000 μg/mL were prepared for each monomer or polymer in methanol and then diluted to prepare samples with different concentrations (1000, 500, 250, 100, 5, and 1 μg/mL). 0.1 mL of these stock solutions were mixed with DPPH solution (30 μg/mL, 2.9 mL) in Eppendorf tubes. The end concentrations in the tubes were 0.3, 1.7, 3.3, 8.3, 16.6, and 33.2 μg/mL of the monomer or polymer samples and 87 μg/mL of DPPH reagent. After incubating the mixtures for 90 min at room temperature in the dark, the absorbance was measured in triplicate at a wavelength of 517 nm using a Perkin Elmer Lambda 365 UV−vis spectrophotometer. The inhibition percentage (I%) was calculated according to the following formula

$$I\% = \left(1 - \left(\frac{(\mathrm{Abs}_{\mathrm{sample}} - \mathrm{Abs}_{\mathrm{blank}})}{(\mathrm{Abs}_{\mathrm{standard}} - \mathrm{Abs}_{\mathrm{blank}})}\right)\right) \times 100$$

where $\mathrm{Abs}_{\mathrm{sample}}$ is the measured absorption of the samples with antioxidants, $\mathrm{Abs}_{\mathrm{blank}}$ is blank with only methanol, and the $\mathrm{Abs}_{\mathrm{standard}}$ is the absorbance of the DPPH without the sample. The start concentration of the antioxidant was plotted against the I%. The IC_{50} values (μg/mL) were calculated by linear fitting the obtained data points. Statistical analysis (t-test) was performed using the SciPy package (stats.ttest_ind).

The same method was used for polymers with the following modifications. All polymers were ground to reduce their particle size and facilitate dissolution. Further, they were sonicated for 15 min using an Ultrasonic Silvercrest SUR 46A1 50 Hz. This ensured the maximum solubility of the polymer in methanol.

Antistatic Activity Measurements. Contact charging of samples was monitored using a method that utilizes a homemade tapping device attached to an oscilloscope. A two-channel oscilloscope was used to independently measure the open-circuit electrical potential (in volts) generated during the contact and separation of the two surfaces. Polymer samples were mounted on aluminum stubs connected to a 100 megaohm (input impedance) oscilloscope probe. The second surface (Al or glass) was mounted on another metal stub attached to an identical probe. The open-circuit voltages (V_{oc}) were measured and collected from saturated signals (signals obtained when accumulated charges are at their maximum values). A 1 Hz tapping frequency was used. Standard deviations were calculated from three independent measurements. The relative humidity during the measurements was 25.6−28.0%. Statistical analysis (t-test) was performed using the SciPy package (stats.ttest_ind).

Synthesis of Dihydroconiferyl Alcohol (DCA). Following a modified literature procedure,[30] under an anhydrous atmosphere, eugenol (18.9 mL, 122.0 mmol) was dissolved in anhydrous THF. The mixture was cooled down to 0 °C, followed by the dropwise addition of borane dimethylsulfide complex (15 mL, 158.2 mmol) over 20 min. After stirring for 1 h at 0 °C, the reaction mixture was

https://doi.org/10.1021/acs.biomac.3c00275
Biomacromolecules 2023, 24, 3498−3509

carefully quenched using water (40 mL). Aqueous sodium hydroxide solution (3 M, 48 mL) was added, and the reaction mixture was again cooled down to 0 °C. Aqueous hydrogen peroxide solution (30%, 28 mL) was added carefully, and the solution was allowed to warm to room temperature, and it was left stirring for 1.5 h. Afterward, the mixture was poured into a beaker and diethyl ether was added, causing the salt to precipitate. The two layers were decanted into a separation funnel, and extractions using diethyl ether were performed. After two extractions, the aqueous solution was acidified using hydrochloric acid, followed by two more extractions using diethyl ether. All organic layers were combined and washed using brine. The solvent was dried using magnesium sulfate, filtered, and removed in a vacuum. The obtained crude product was purified by recrystallization in a dichloromethane/petroleum ether (1:5) mixture. Off-yellow crystals were obtained in a 73% yield and a 95% isomer purity. ^{1}H NMR (400 MHz, $CDCl_3$; Figure S1) δ 6.83 (d, J = 7.9 Hz, 1H), 6.72−6.67 (m, 2H), 3.87 (s, 3H), 3.68 (t, J = 6.4 Hz, 2H), 2.64 (t, J = 7.6 Hz, 2H), 1.87 (tt, J = 7.6, 6.4 Hz, 2H).

Selective (Meth)Acrylation of DCA. The transesterification was performed by combining DCA (3 mmol, 547 mg) and methyl acrylate or methyl methacrylate (12 mmol) in an oven-dried vial. Next, the radical inhibitors 4-methoxyphenyl (0.05 wt %) and phenothiazine (0.05 wt %) were added together with Novozym 435 (10 wt %, immobilized, 10,000 PLU/g). Finally, molecular sieves of 5 Å were added to remove methanol and to allow complete conversion to be reached. The reaction was gently shaken for 24 h at 60 °C to ensure complete conversion for all aliphatic alcohols (followed by thin-layer chromatography (TLC)). The crude reaction mixture was dissolved in dry THF, and the immobilized enzyme and molecular sieves were filtered off. Residual methanol and methyl (meth)acrylate are removed under a vacuum. The final mono-(meth)acrylated DCA was obtained in moderate to good yields (71−89%) with purity over 95%. The compounds were stored at 4 °C under a N_2 atmosphere until used.

Methacrylated DCA (DCAMA). ^{1}H NMR (400 MHz, $CDCl_3$, δ (ppm); Figure S3): 6.82 (d, J = 8.5, 1H), 6.69−6.65 (m, 2H), 6.10 (dd, J = 1.8, 0.9 Hz, 1H), 5.56 (dd, J = 1.6, 0.7 Hz, 1H), 4.15 (t, J = 6.5, 0.7 Hz, 2H), 3.86 (s, 3H), 2.63 (t, J = 6.8 Hz, 2H), 2.01−1.96 (m, 1H), 1.94 (dd, J = 1.6, 0.8 Hz, 3H). LC−MS (Figure S4) m/z calcd. for $C_{14}H_{18}O_4$ H− 249.1132; found: 249.1141.

Acrylated DCA (DCAA). ^{1}H NMR (400 MHz, $CDCl_3$, δ (ppm); Figure S5): 6.82 (d, J = 8.5 Hz, 1H), 6.71−6.62 (m, 2H), 6.40 (ddd, J = 17.3, 1.5, 0.5 Hz, 1H), δ6.13 (ddd, J = 17.3, 10.4, 0.5 Hz, 1H), 5.82 (ddd, J = 10.4, 1.4, 0.5 Hz, 1H), 4.17 (t, J = 6.5 Hz, 2H), 3.85 (s, 3H), 2.63 (t, J = 8.6, 6.8 Hz, 2H), 2.02−1.90 (m, 2H). LC−MS (Figure S5) m/z calcd. for $C_{13}H_{16}O_4$ H− 235.0976; found: 235.0982.

RAFT Copolymerization of HEMA and DCAMA or HBA and DCAA. The RAFT copolymerizations of DCAMA with HEMA and DCAA with HBA were performed using the RAFT agent CDP-TTC and AIBN as the initiator in a ratio of 1:0.4 molar using DMF as a solvent. The total monomer concentration is 1.4 M. A series of copolymerizations were performed, whereby the monomer to CTA molar ratios, initial HEMA or HBA concentration, and initial DCAMA or DCAA concentration are varied (Tables S1 and S2). In a typical copolymerization, all components (AIBN, CDP-TTC, uninhibited HEMA or HBA, and DCAMA or DCAA) were dissolved in uninhibited DMF (filtered over activated, basic aluminum oxide, Brockmann type I) in a 10 mL Schlenk flask containing a magnetic stirring bar and closed by rubber septa. The reaction mixture was degassed by three freeze−pump−thaw cycles and kept under an argon atmosphere (purity 99.999%). The Schlenk flask was placed at 70 °C for the times specified in Tables S1 and S2, and periodic sampling of the reaction is accomplished with an argon-flushed syringe. Part of the sampling volume (25 μL) was diluted in DMSO-d_6 (0.6 mL) and subsequently used to determine the monomer conversion by ^{1}H NMR. The leftover sampling volume (150 μL) was quenched by adding hydroquinone (5 mg) and stored for further analysis with GPC.

Synthesis of Poly(HEMA-*co*-DCAMA)-*b*-*p*BMA Diblock Terpolymers. The synthesis of poly(HEMA-*co*-DCAMA)-*b*-BMA diblock terpolymers was conducted using the above-synthesized poly(HEMA-*co*-DCAMA) macroCTA for the chain extension with BMA. In a 50 mL Schlenk flask equipped with a magnetic bar, poly(HEMA-*co*-DCAMA) macroCTA (0.2 g), BMA (0.09 g, 0.65 mmol), AIBN (1 mg, 6.55×10^{-3} mmol), and DMF (1.5 mL) were transferred. The reaction mixture was stirred for 20 min at an ambient temperature and deoxygenated by three freeze−pump−thaw cycles, and the flask was placed in a preheated oil bath at 70 °C for 6 h. The polymerization was terminated by immersing the flask in liquid nitrogen and opening it to air. The product mixture was precipitated from chilled water and was recovered by centrifugation and finally dried under vacuum at 40 °C overnight to yield white crystals (0.25 g, yield = 86%). The terpolymer was characterized by ^{1}H NMR spectroscopy for the determination of the molar composition and by GPC for the estimation of molar masses. Two diblock terpolymers with different compositions and molar masses were synthesized by varying the $[BMA]_o/[poly(HEMA\text{-}co\text{-}DCAMA)macroCTA]_o$ molar ratio. This polymerization procedure yielded a poly(HEMA-*co*-DCAMA)-*b*-*p*BMA diblock terpolymer containing 33.2 mol % PBMA, with M_n = 13,900 g/mol and $Đ$ = 1.29. Using the same procedure, another diblock terpolymer poly(HEMA-*co*-DCAMA)-*b*-*p*BMA block terpolymer containing a higher PBMA molar composition (47.8 mol % PBMA) with M_n = 15,500 g/mol and $Đ$ = 1.27 was synthesized. The nomenclature and composition of diblock terpolymers are shown in Table S3.

Determination of Reactivity Ratios of HEMA with DCAMA and HBA with DCAA. To determine the reactivity ratios of HEMA and DCAMA, eight copolymerizations with different monomer feed compositions were performed by free-radical polymerization. The molar fraction of DCAMA in the feed (f_{DCAMA}) ranged from 10 to 80 mol % (Table S4). Predetermined amounts of monomers, AIBN as a free-radical initiator, and DMF as a solvent were weighted in a Schlenk flask equipped with a magnetic bar. The Schlenk flask was closed by a rubber septum, degassed by three freeze−pump−thaw cycles, and kept under an argon atmosphere. In all cases, the concentration of monomers to solvent was kept constant at 0.33 g/mL to ensure similar polymerization conditions for all reaction mixtures. Finally, the copolymerization was triggered by immersing the flask in a preheated oil bath at 70 °C. All reaction mixtures were stirred for 10 min, and the copolymerizations were quenched by immersing the flask in liquid nitrogen and then opening it to air to ensure that the monomer conversion was lower than 10%. The total product mixture was purified by precipitation into a 15-fold volume of excess chilled diethyl ether, recovered by centrifugation, and dried under vacuum at 40 °C. The molar fraction of DCAMA in the copolymer (F_{DCAMA}) was determined by ^{1}H NMR in DMSO-d_6.

The reactivity ratios were determined by applying mathematical models of copolymerization, which correlate the relationship between the composition of the monomer feed and the composition of the copolymers. In the present study, Fineman−Ross,[31] Kelen−TÜdos,[32] and Mayo−Lewis[33] curve fitting methods were applied for the accurate calculation of reactivity ratios. The former is expressed by eq 1

$$G = H \times r_1 - r_2 \tag{1}$$

By plotting $G = f_1(2F_1 - 1)/(1 - f_1)F_1$ as ordinate versus the $H = f_1^2(1 - F_1)/(1 - f_1)^2F_1$ as abscissa yields a straight line where the slope is the value of r_1 and the intercept is the value of $-r_2$. The Kelen and TÜdos method employs the following equation

$$\eta = [r_1 + r_2/\alpha]\mu - r_2/\alpha \tag{2}$$

This involves η and ζ parameters, which are mathematical functions related to the mole ratios in the monomer feed and the copolymer and an arbitrary constant α. The parameters are defined as $\eta = G/(a + H)$, $\mu = H/(\alpha + H)$, and $a = (H_{max}H_{min})^{0.5}$, where H_{min} and H_{max} are the highest and lowest values of H from the Fineman−Ross method, respectively. Thus, a plot of η against μ gives a straight line that can be extrapolated at μ = 0 and μ = 1, thereby yielding the respective η intercepts. The Mayo−Lewis fitting curve method applies the Mayo−Lewis copolymerization (eq 3) using the least-squares method to a

https://doi.org/10.1021/acs.biomac.3c00275
Biomacromolecules 2023, 24, 3498−3509

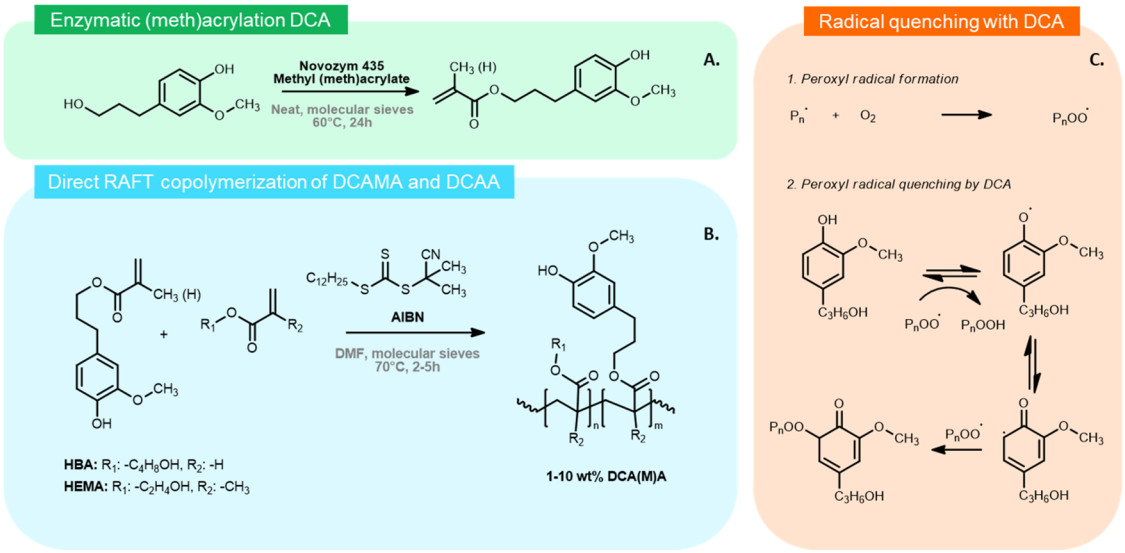

Figure 2. (A) Lipase-catalyzed transesterification of DCA and methyl (meth)acrylate for the selective (meth)acrylation of the primary hydroxyl group. (B) RAFT homo copolymerization of DCAMA or DCAA with HEMA or HBA at different degrees of polymerizations and mass fractions of DCAMA or DCAA. (C) Peroxyl radical formation of a growing polymer chain (P_n) with oxygen and its subsequent quenching by DCA.

composition diagram of the incremental DCAMA copolymer composition as a function of the monomer composition for different reactivity ratios

$$F_1 = (r_1 f_1^2 + f_1 f_2)/(r_1 f_1^2 + 2 f_1 f_2 + r_2 f_2^2) \quad (3)$$

where F_1, f_1, f_2, r_1, and r_2 stand for the molar fraction of DCAMA in the copolymer; the molar fraction of DCAMA and HEMA in the comonomer feed, and the reactivity ratios of DCAMA and HEMA, respectively.

RESULTS AND DISCUSSION

Lipase-Catalyzed Selective (Meth)Acrylation of DCA. Dihydroconiferyl alcohol (DCA) was synthesized based on a modified literature[30] procedure to yield a pure starting material after recrystallization. DCA can also be obtained from depolymerized lignin oil as we and other researchers showed in previous reports through solvent fractionation techniques.[34] Typically, the acryl and methacryl-esterification of lignin-derived phenolic compounds (monolignols) have used reactive and toxic compounds such as acryloyl or methacryloyl chloride.[17] These reagents achieve high yields but are not selective toward either aliphatic or phenolic hydroxyl groups, with diacrylate DCA as a result. Furthermore, extensive purification is needed to remove impurities. Less reactive acrylation reagents such as methacrylic anhydride will lead to fewer side products with less elaborate purification protocols required. Still, no selectivity of the aliphatic hydroxyl group over the phenolic hydroxyl group for the esterification of DCA or other monolignols can be obtained. This is unfortunate as it is well established that the functionality of lignin, such as its UV-blocking, flame-retardance, antioxidant (AA), and anti-static properties, is at least in part dependent on the availability of free phenolic hydroxyl groups.[35]

To that end, an enzymatic strategy was developed to selectively acrylate and methacrylate the primary hydroxyl group of DCA using methyl acrylate (MA) and methyl methacrylate (MM). Novozym 435 (N435) is a commercially available immobilized lipase B from Candida Antarctica on a Lewatit VP OC 1600 resin.[25] N435 is one of the most widely used commercial biocatalysts in both academia and industry and is known to catalyze transesterification reactions under mild conditions. Several green chemistry principles are fulfilled in the developed method. The synthesis proceeds at 60 °C under neat conditions with only DCA, methyl acrylate or methyl methacrylate, and N435 required. After shaking for 24 h, DCA conversions up to 95% are reached for both DCAMA (methacrylated DCA) and DCAA (acrylated DCA) (see Figure S2 for transesterification kinetics of both DCAMA and DCAA). The immobilized N435 enzyme is simply removed by filtration, and pure DCAMA (Figures S3 and S4) or DCAA in a 95% yield (Figures S5 and S6) was obtained after the removal of the residual methyl (meth)acrylate and methanol by distillation.

RAFT Copolymerization of DCAMA and DCAA. The mono-acrylated DCA monomers DCAMA and DCAA (Figure 2B) were copolymerized with commercially available monomers such as HEMA (2-hydroxyethyl methacrylate) and HBA (4-hydroxybutyl acrylate). Thermal RAFT polymerization was employed to not only obtain copolymers with targeted molar masses and narrow dispersities but also investigate the influence of the mono-acrylated DCA monomers and their potential radical scavenging ability on the overall polymerization process and molar mass distribution. The kinetics of RAFT polymerizations and controlled radical polymerization (CRP), in general, are well studied and known.[36] Deviation from the ideal polymerization behavior could give insights into the radical quenching effect of DCA. Therefore, an in-depth kinetic study was performed, whereby different degrees of polymerization were targeted and the mass fraction of the DCA-derived acrylate was varied. Additionally, the copolymerization ratios of DCAMA with HEMA and DCAA with HBA were determined, which yields insights into the copolymer composition. The polymerization and monomer conversion were tracked with ^{1}H NMR after taking aliquots at distinct reaction times, while the molecular weight evolution was followed by GPC.

The RAFT polymerization is conducted in the following way: the cyano-RAFT agent is dissolved in DMF, together with the monomers and thermal initiator (AIBN) in DMF (Tables

https://doi.org/10.1021/acs.biomac.3c00275
Biomacromolecules 2023, 24, 3498−3509

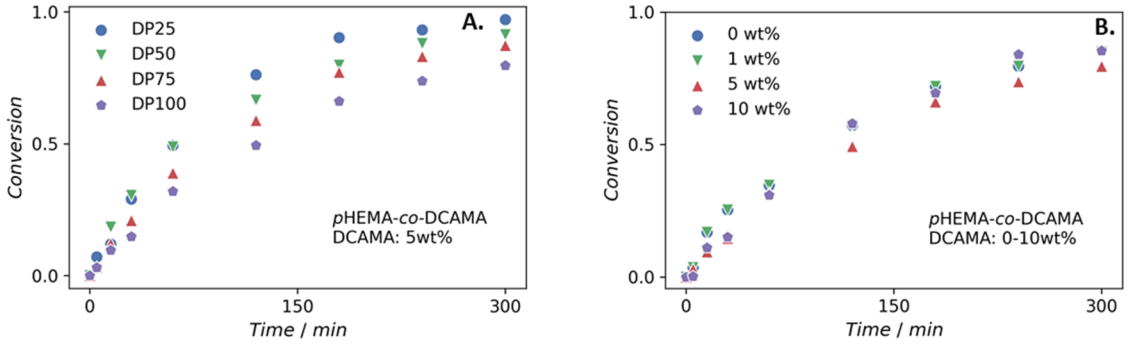

Figure 3. (A) Monomer conversion vs time kinetics plot of the RAFT copolymerization of HEMA and DCAMA (5 wt %) for target DP25-100. (B) Monomer conversion vs time kinetics plot of the RAFT copolymerization of HEMA and DCAMA (0−10 wt %) for target DP100.

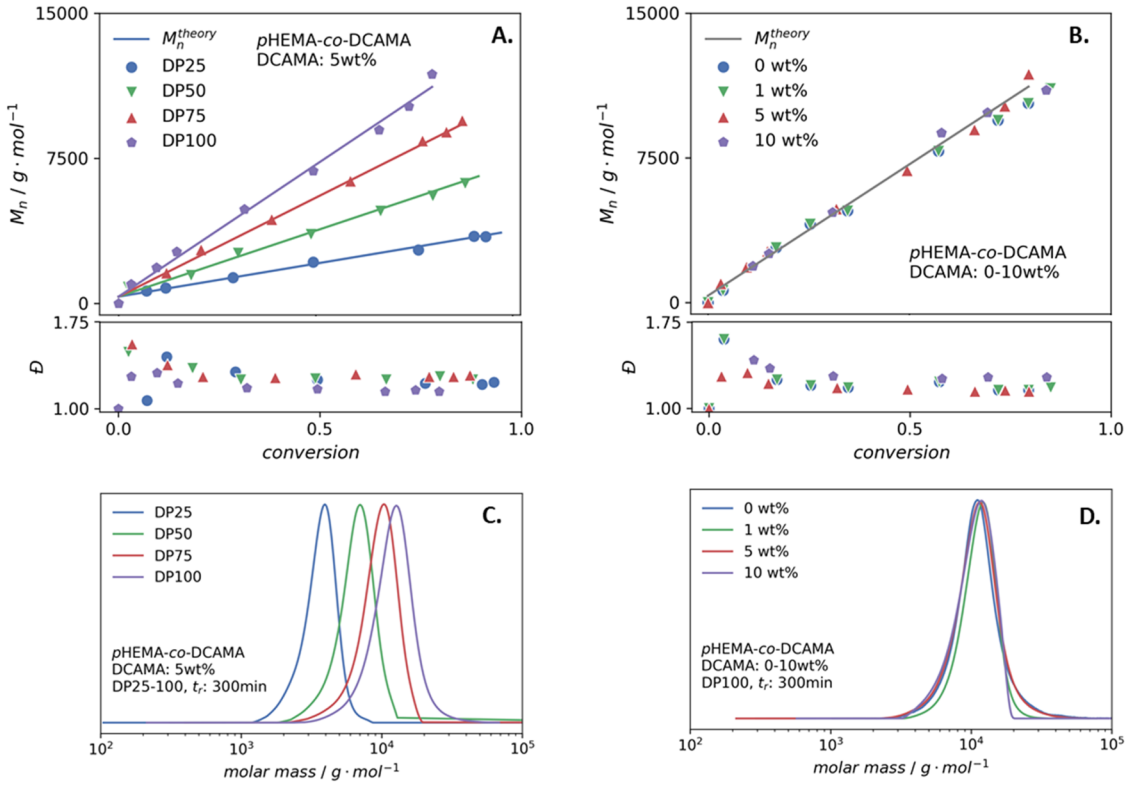

Figure 4. (A) Number-average molar mass and dispersity as measured by GPC as a function of the overall monomer conversion at different DPs for the copolymerization of DCAMA (5 wt %) with HEMA. (B) Number-average molar mass and dispersity as measured by GPC as a function of the overall monomer conversion for DP100 at different weight fractions of DCAMA (0, 1, 5, and 10 wt %) for the copolymerization with HEMA. (C) Molar mass distributions at maximum conversion for the copolymerization of DCAMA (5 wt %) with HEMA at DP25, 50, 75, and 100. (D) Molecular weight distributions at maximum conversion for the copolymerization of DCAMA at different weight fractions (0, 1, 5, and 10 wt %) with HEMA for target DP100.

S1 and S2). Next, oxygen is removed from the polymerization mixture by three cycles of freeze−pump−thaw, and the polymerization is conducted under an argon atmosphere at 70 °C. Minimizing the oxygen content in the reaction mixture is crucial for the polymerization to proceed. As shown in Figure 2C, hindered phenol acts as a radical scavenger of peroxyl radicals, which are formed from carbon-centered radicals (like growing polymer chains) that react with oxygen.[37] In theory, when limiting the oxygen content, the radical polymerization should proceed without any inhibition or influence on the RAFT equilibrium.

Despite the radical scavenging ability of DCAMA and DCAA, the RAFT copolymerization produced successful copolymers over a wide range of monomer compositions and monomer conversions. Overall, monomer conversions up to 95% were reached after only 6 h of reaction time (Figure 3A) for the copolymerization of DCAMA (5 wt %) with HEMA at a target degree-of-polymerization (DP) of 25. Increasing the DP stepwise from 25 to 50, 75, and 100 does show a slight decrease in monomer conversion (Figure 3A), but still monomer conversions over 85% are attained. This shows that the radical polymerization is not limited in a significant manner by the presence of the DCA-derived monomers containing free phenolic hydroxyl groups.

The RAFT-to-AIBN molar ratio is fixed at 1:0.4; hence, lowering the RAFT agent concentration also lowers the radical concentration and the overall polymerization rate. More importantly, even when 10 wt % of DCAMA monomer is

https://doi.org/10.1021/acs.biomac.3c00275
Biomacromolecules 2023, 24, 3498−3509

present in the feed, no significant difference in the polymerization rate is found when compared to the homopolymerization of HEMA (Figure 3B). A 10 wt % of DCAMA corresponds with a 14-fold molar excess of phenolic hydroxyl groups to the total amount of radicals that can be formed, assuming complete initiator conversion. During the polymerization, the overall radical concentration will be orders of magnitude lower than the free phenolic concentration due to radical chain termination events and slow initiator decay. Even though this large molar excess of free phenolic from DCA-derived monoacrylate, polymerization occurs uninhibited.

As seen in Figure 4, the RAFT copolymerization of DCAMA with HEMA for multiple target DP's and weight fractions of DCAMA proceeds in a well-controlled fashion, whereby a linear correlation is found between the monomer conversion and molecular weight evolution. This good control over the polymerization is also observed via the GPC traces, with no low or high molar mass tailing visible. Furthermore, the obtained number-average molar masses (M_n) agree with their theoretical values, and the dispersity values remain low ($Đ$ <1.35) for high monomer conversions. These results indicate that the chain-transfer constant of the cyano-trithiocarbonate RAFT agent is orders of magnitude higher than the one of the phenols, which is also consistent with literature reports.

The RAFT polymerization between DCAA and HBA was also studied similarly to DCAMA and HEMA. The same CDP-TTC raft agent was used with the same RAFT-to-initiator ratio of 1:0.4, and all other experimental conditions and procedures were kept the same. (see Table S2 for experimental details). With these conditions of the RAFT-mediated polymerization, an inhibition period was observed, even for the homopolymerization of HBA (Figure S21A). Increasing the weight fraction of DCAA with 1 and 5 wt % did not change the overall kinetics with similar steady-state radical concentrations as observed in the first-order kinetics plot (Figure S21B). When increasing the DCAA content to 10 wt %, a decrease in the apparent polymerization rate was observed, with only 70% conversion reached after 120 min, while for 0, 1, and 5 wt % of DCAA, monomer conversions of 90% were obtained. Similarly, a lower steady-state radical concentration was found in the first-order-kinetics plots. Hindered phenols are known to act as retarders for the polymerization of acrylates at low amounts of oxygen in the reaction mixture, while at higher levels of oxygen, they act as inhibitors. As shown by Cutié et al.,[38] this mechanism of retardation of acrylate polymerization by phenols appears to act through the direct interaction with the initiator fragments and not by the irreversible termination of the growing polymer chains. Hence, the retardation effect only influences the overall polymerization rate and not the final molecular weight distribution of the polymer. This effect was also indeed observed in the RAFT-mediated copolymerization of DCAA with HBA. While the overall reaction rate is lowered with an increase in the DCAA content, the final obtained polymers showed a well-defined molecular weight distribution and a linear increase in number-average molecular weight with conversion (Figure S22).

Synthesis of Poly(HEMA-*co*-DCAMA)-*b*-*p*BMA Diblock Terpolymers by Chain Extension from Poly(HEMA-*co*-DCAMA) MacroCTA. The well-defined molecular weight distributions showing low dispersities as well as the good agreement between theoretical and experimental molar masses are solid evidence of a well-controlled RAFT polymerization process. Still, to further demonstrate that poly(HEMA-*co*-DCAMA) copolymers with high-end-group fidelity are obtained, sequential polymerization of BMA was performed. Additionally, it is essential to explore the limitation of poly(HEMA-*co*-DCAMA) copolymers to serve as macroinitiators as irreversible termination through the grafting of the DCA structure can result in low-molecular-weight tailing. Therefore, block copolymers containing PBMA segments of various lengths were prepared, under identical experimental conditions, by varying the [BMA]/[macroinitiator] molar ratio charged in the polymerization. The successful synthesis of these diblock terpolymers was evidenced by GPC and ^{1}H NMR spectroscopy, and the results are summarized in Table S3.

Figure 5 displays the chromatograms of the poly(HEMA-*co*-DCAMA)-*b*-*p*BMA diblock terpolymers. The unimodal GPC traces of the diblock terpolymers shifted toward lower elution times, indicating an increase in molar mass during the polymerizations of BMA. Moreover, no significant tailing of the molecular weight distributions was observed, resulting in almost no broadening of the distributions of the block copolymers.

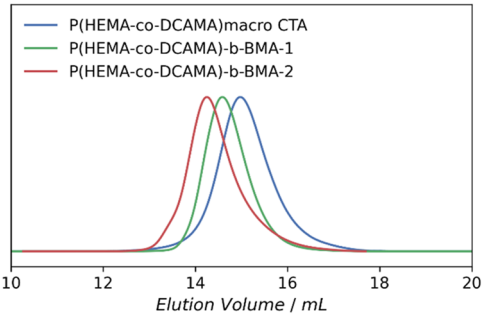

Figure 5. Normalized GPC traces of the diblock terpolymers derived from (poly(HEMA-*co*-DCAMA)) macroCTA.

Diblock terpolymers were analyzed by ^{1}H NMR spectroscopy to obtain their compositions. Figure S34 depicts the ^{1}H NMR spectra of the poly(HEMA-*co*-DCAMA) macroinitiator where resonances assigned to both the DCAMA and HEMA comonomers were observed. Especially, the doublet between 6.5 and 7.0 ppm was assigned to the aromatic's proton of DCAMA, while the peak appeared at 4.8 ppm corresponding to the methylene protons adjacent to carbonyl groups of HEMA. However, in the case of the diblock terpolymers (Figure S35), resonances associated with PBMA units were not visible due to their similar molecular structure to the DCAMA and HEMA. The signal intensity corresponding to the PBMA block was calculated by subtracting the signal intensity in the region ranging from 0.5 to 1.2 ppm, assigned to methyl protons of DCAMA, HEMA, and BMA, from the intensity in the corresponding region of poly(HEMA-*co*-DCAMA) macroinitiator. The molar composition of BMA was calculated from the ratio of these peaks, which was in good agreement with the comonomer composition in the feed, as can be seen in Table S3, which verifies our assumption that indeed the first block has a high-end-group fidelity, with complete reinitiation and little irreversible termination occurring.

Copolymerization Reactivity Ratios of DCAMA with HEMA and DCAA with HBA. To the best of our knowledge, (co)polymerization of DCAMA or DCAA has not been reported before. To predict the composition of the final

https://doi.org/10.1021/acs.biomac.3c00275
Biomacromolecules 2023, 24, 3498−3509

copolymer, we determined the reactivity ratios for the free-radical polymerization of DCAMA with HEMA and DCAMA with HBA at 70 °C in DMF. For that purpose, free-radical polymerizations with feeds ranging from 11 to 92 mol % DCAMA and DCAA were conducted and were quenched at low conversion (<10%) to avoid a composition drift, and the molar fraction of each comonomer in the copolymer was then calculated by ^{1}H NMR spectroscopy, as indicated above (Table S4). Figure 6C presents the composition diagram of the

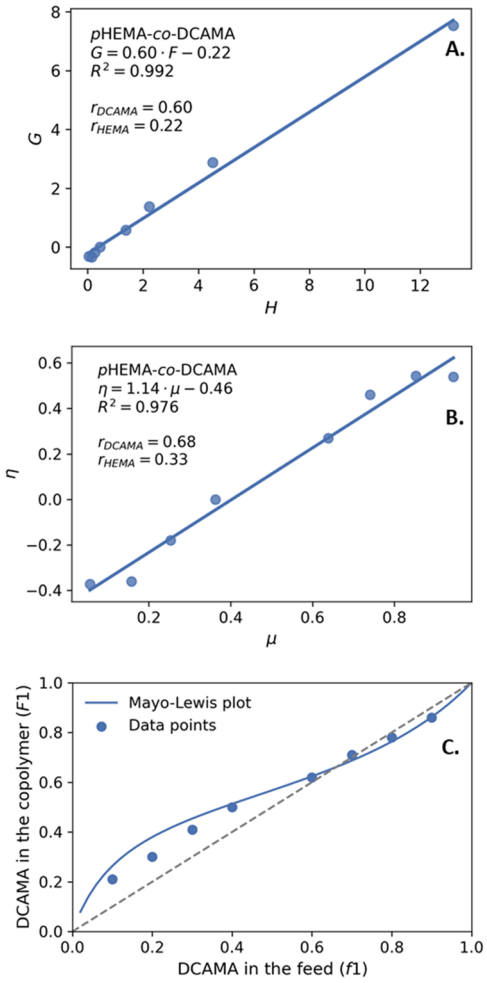

Figure 6. Determination of the reactivity ratios of DCAMA and HEMA in DMF at 70 °C by free-radical polymerization: (a) Fineman−Ross (FR), (b) Kelen−TÜdos (KT), and (c) Mayo−Lewis plots using experimental reactivity ratio. The blue solid line represents the theoretical curve calculated from the copolymer composition equation using experimental reactivity ratios, which are in line with the experimental copolymer composition data (blue circle points). The dashed straight line indicates the azeotropic composition, where $F_{DCAMA} = F_{HEMA}$.

DCAMA molar fraction in the copolymer (F_{DCAMA}) vs its molar fraction in the feed (f_{DCAMA}). The proposed linearization methods by Fineman−Ross (FR, Figure 6A) and the Kelen−TÜdos (KT, Figure 6B) were used for the determination of the reactivity ratios (r_{DCAMA}, r_{HEMA}). Reactivity ratios obtained by these methods were consistent, with the average values being $r_{DCAMA} = 0.64 \pm 0.05$ and $r_{HEMA} = 0.28 \pm 0.08$, suggesting that DCAMA is slightly more reactive than HEMA. The reactivity ratios varied between 0 and 1 but not ≪1; therefore, the tendency toward alternation is not highly pronounced in their copolymers; instead, the formation of random copolymer is favored with a slight gradient in composition along the backbone of the copolymer. Comparable results were found for the copolymerization of DCAA with BMA, the average values being $r_{DCAA} = 0.70 \pm 0.1$ and $r_{HEMA} = 0.20 \pm 0.04$, suggesting the formation of a random copolymer structure (Figure S36).

Antioxidative Properties. It is well known that lignin-derived monomers (monolignols) have strong antioxidant activity (AA) due to the presence of freely available phenolic hydroxyl groups.[39] Other elements of their structure determine the extent of the AA. DCA was the monomer of interest due to its availability in high quantities from softwood depolymerized lignin oils, and the aliphatic handle allows further functionalization. The antioxidative properties of DCA and (meth)-acrylated DCA, DCAMA, and DCAA were measured and compared with the commercial antioxidant (BHT) for benchmarking (Figure 7A). The radical scavenging activity

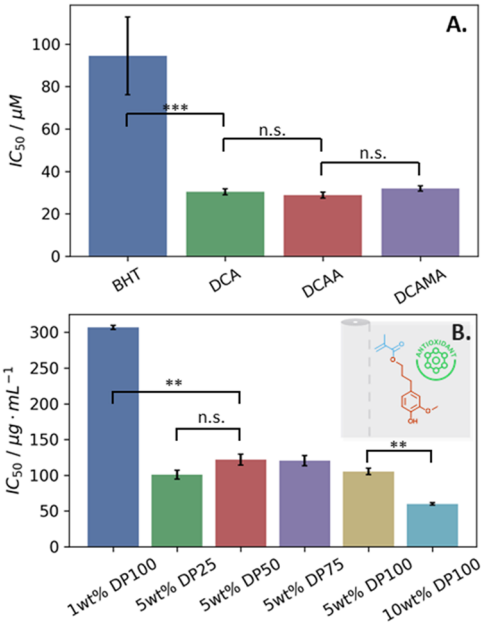

Figure 7. (A) Radical scavenging ability (IC_{50}) of the compounds BHT, DCA, DCAA, and DCAMA. (B) Radical scavenging ability (IC_{50}) of the poly(HEMA-*co*-DCAMA) copolymers with different amounts of DCAMA and various chain lengths. The lower the IC_{50} value, the stronger the antioxidant activity. Error bars correspond to standard deviations determined from at least two measurements. Statistical significances determined by *T*-test. A *p*-value of less or equal to 0.001 is represented by ***, a *p*-value of less or equal to 0.01 is represented by **, a *p*-value of less or equal to 0.05 is represented by *, and a *p*-value larger than 0.05 is considered not significant (n.s.).

was determined by the 2,2-diphenyl-1-picrylhydrazyl radical (DPPH) assay. The results are expressed as an IC_{50} value, which is the required antioxidant concentration to inhibit 50% of the DPPH radicals in the assay. The lower the IC_{50} value, the stronger the antioxidant activity.

The IC_{50} of DCA was determined to be 32 μM, in line with previously reported data.[2] Furthermore, the acrylated (DCAA) and methacrylated (DCAMA) derivates show almost identical IC_{50} values, with 30 and 33 μM, respectively. This indicates that the modification of the aliphatic hydroxyl group does not influence the radical scavenging ability of the monolignol.

https://doi.org/10.1021/acs.biomac.3c00275
Biomacromolecules 2023, 24, 3498−3509

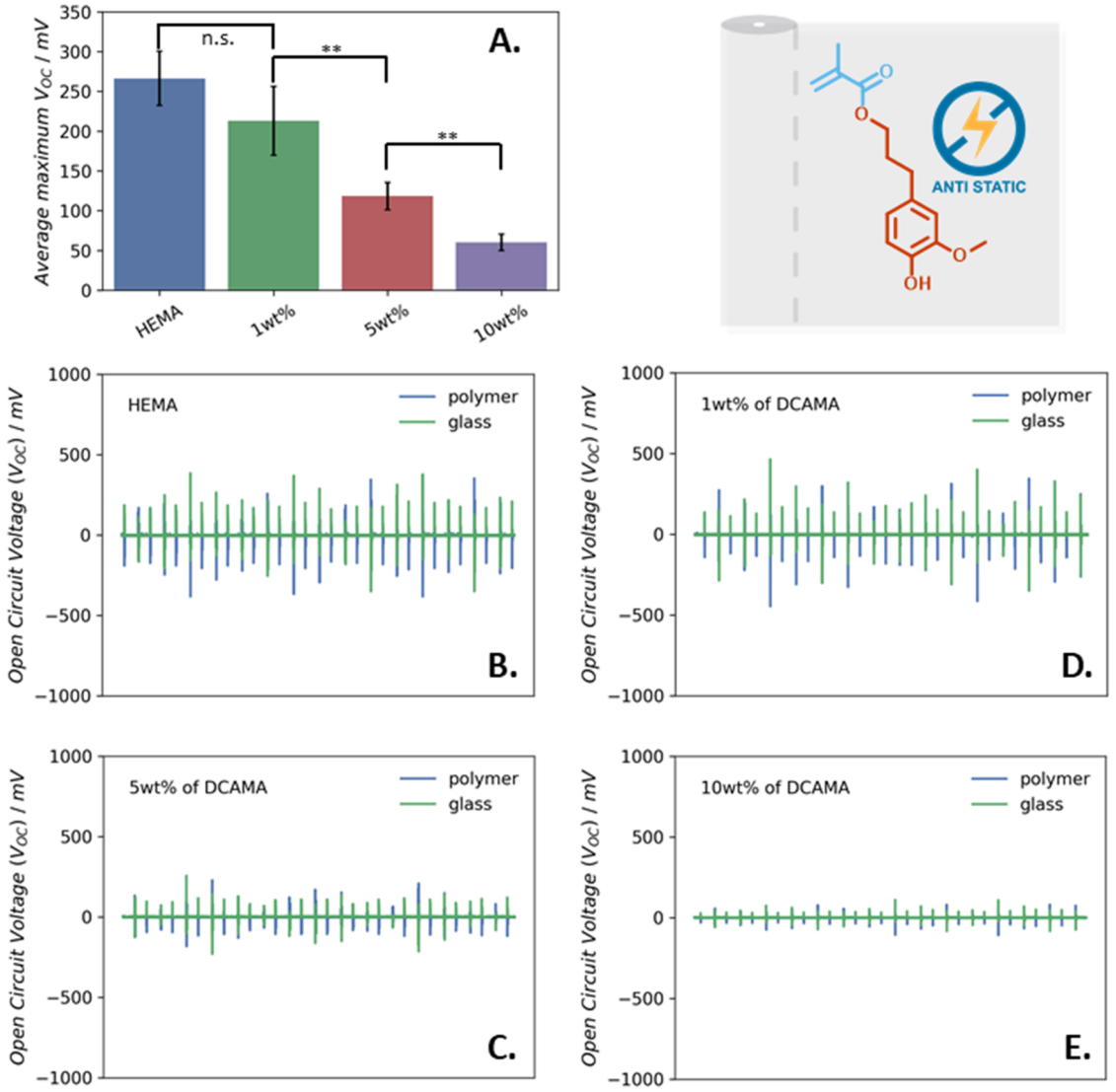

Figure 8. (A) Average open-circuit potentials (V_{oc}) obtained by tapping samples on glass versus concentration of DCAMA in the polymer. Error bars correspond to standard deviations determined from at least three independent measurements. Statistical significance is determined by *T*-tests. A *p*-value of less or equal to 0.001 is represented by ***, a *p*-value of less or equal to 0.01 is represented by **, a *p*-value of less or equal to 0.05 is represented by *, and a *p*-value larger than 0.05 is considered not significant (n.s.) (B–D). Average V_{oc} obtained by tapping reference samples and DCAMA containing samples on glass and polymer.

Interestingly, the radical scavenging ability of DCA and its (meth)acrylated derivates are more than double that of the commercial antioxidant BHT (79 μM), which is commonly used as a food additive and in personal care products. BHT is a suspected carcinogen, and the U.S. Food and Drug Administration (FDA) has therefore restricted its use.[40] These results also indicate that the methoxy group, characteristic of lignin, is a better radical stabilizer than the *tert*-butyl group commonly used in synthetic fossil-derived antioxidants.

The same DPPH assay was used to determine the antioxidant properties of the poly(HEMA-*co*-DCAMA) copolymers synthesized using RAFT polymerization, as described in the previous section. As expected, the benchmark poly(HEMA) shows no antioxidant properties. However, incorporating as little as 1 wt % of DCAMA into the polymer backbone resulted in antioxidant activity. This activity increases with an increasing amount of DCAMA and does not show any dependency on the molecular weight of the copolymer (Figure 7B). When calculating the theoretical 100 wt % equivalents instead of 1, 5, and 10 wt %, their AA shows a range of 3–6 $\mu g \cdot mL^{-1}$ for the IC_{50} value. These experimental results are in remarkably close agreement with the IC_{50} values of DCAMA (8 $\mu g \cdot mL^{-1}$). This indicates that the AA of the DCA (meth)acylated monomers remains without any loss in performance after polymerization.

Antistatic Properties. Contact electrification (CE) is the development of surface charges upon contact and separation, which result in the buildup of an electrical potential. Static electricity is a serious challenge in many industries, notably in the microelectronics sector where billion-dollar losses are associated each year with the failure of electronic components and semiconductor devices damaged by electrostatic discharge (ESD). Baytekin et al.[41] demonstrated that an efficient way to remove static electricity (and thus discharge) from a polymer is to remove the radicals from its surface. A practical consequence of this charge-radical equivalence is that insulating polymers could readily be made antistatic by simply doping them with a small number of radical scavengers.

https://doi.org/10.1021/acs.biomac.3c00275
Biomacromolecules 2023, 24, 3498–3509

Baytekin et al. further expanded this concept by designing antistatic commodity plastics incorporating lignin particles as additives and demonstrated that the strong antistatic action could be linked to the presence of free phenolic groups on the lignin structure.[7]

The same phenolic structures as in lignin are also present in the DCA-derived monomers, and any polymer containing such DCA monomers should in theory be effective in charge dissipation by making the surface of the polymer material antistatic. To that end, three different poly(HEMA-*co*-DCAMA) polymer films with 1, 5, and 10 wt % of DCAMA were manufactured by solvent casting method. As a benchmark, a poly(HEMA) film was made, and all films were analyzed for their antistatic nature by contact charge monitoring under repeated tapping of a polymer-mounted electrode to a glass-mounted electrode. A 1 Hz tapping frequency was used, and the open-circuit voltages (V_{oc}) were measured and collected from saturated signals (signals obtained when accumulated charges are at their maximum values). As shown in Figure 8, the addition of lignin-derived acrylic monomer (DCAMA) into the polymers reduces the electrostatic potential developed on the polymer surface upon contact charging compared to the reference sample (poly-HEMA). This outcome is in line with the fact that the antistatic effect of lignin is a result of the phenolic groups in its structure. To the best of our knowledge, this is the first example whereby an insulating homopolymer also exhibits a strong antistatic effect without adding additional additives. The classical approach to making plastics more antistatic is by incorporating additives to make the material more conductive (e.g., by doping with metals, carbon powders, or blending with conductive polymers).[42] On the other hand, most insulators create surface charges upon contact. Therefore, the poly-(HEMA-*co*-DCAMA) polymers synthesized in this work show unique properties as they are both an insulator (non-conductive) and antistatic.

CONCLUSIONS AND OUTLOOK

In summary, the work described herein shows that lignin-derived monomers can be used to synthesize well-defined acrylic polymers with strong antioxidant and antistatic properties. Using the developed enzyme-catalyzed process, bifunctional monolignol (DCA) containing both aliphatic and phenolic hydroxyl groups was selectively (meth)acrylated at the aliphatic hydroxyl group using green chemistry principles. Contrary to the standard approach of using additives to give functionality to polymers, we have shown that the direct (without protecting the phenolic hydroxyl group to limit its radical scavenging ability) free-radical or RAFT copolymerization of monomers with radical scavenging functionality can be performed while maintaining control over the incorporation of the lignin-derived monomers and the overall molecular weight distribution, respectively. High monomer conversions (over 85%) and low dispersities (<1.35) were obtained. This indicates that the radical polymerization can proceed uninhibited in the presence of radical scavenging monomers when the oxygen content is kept to a minimum. Furthermore, the copolymerization ratios of both the methacrylated and acrylated DCAs (DCAMA and DCAA) were experimentally obtained for the copolymerization with hydroxyethyl methacrylate (HEMA) and hydroxybutyl acrylate (HBA). It was found that DCAMA and DCAA were slightly more reactive than HEMA and HBA, respectively, leading to a slight gradient in composition along the backbone of the copolymer.

A DPPH assay determined the radical scavenging properties and antioxidative activity of DCA and DCA-derived (meth)-acrylates. It was found that the modification of DCA at the aliphatic alcohol does not diminish the antioxidative activity. Furthermore, the antioxidative activity of DCA and DCA-derived (meth)acrylates is more than 2 times higher than those of commercial antioxidants such as BHT. Upon copolymerization, the antioxidant activity remains without any decrease compared to the isolated monomers. Additionally, antistatic testing indicates that similar performance can be achieved with lignin-doped common plastics. This results in a unique material that is an insulator and antistatic. Hence, these polymers show interesting properties for both bulk and niche applications, for instance, as a food-packaging material. Avoiding the leaching of additives in these acrylic films is crucial for both preserving food and preventing the consumption of harmful chemicals. Additionally, being both an antistatic and insulating material shows promising use cases for microelectronics and other areas where static charge buildup is unwanted.

ASSOCIATED CONTENT

Data Availability Statement

The raw data required to reproduce these findings are available to download upon request from VITO. The processed data required to reproduce these findings are available in the Supporting Information, including the relevant processing scripts.

Supporting Information

The Supporting Information is available free of charge at https://pubs.acs.org/doi/10.1021/acs.biomac.3c00275.

Data concerning the GPC, NMR, and DPPH assays and their data processing; summary of poly(HEMA-*co*-DCAMA) synthesized with thermal RAFT polymerization; and free-radical copolymerization of DCAMA with HEMA and DCAA with BMA for determining reactivity ratios (PDF)

AUTHOR INFORMATION

Corresponding Author

Maarten Rubens − *Flemish Institute for Technological Research (Vito N.V.), Mol 2400, Belgium;* orcid.org/0000-0003-2859-5766; Phone: +32 14 33 57 81; Email: maarten.rubens@vito.be

Authors

Panagiotis Falireas − *Flemish Institute for Technological Research (Vito N.V.), Mol 2400, Belgium*

Karolien Vanbroekhoven − *Flemish Institute for Technological Research (Vito N.V.), Mol 2400, Belgium*

Wouter Van Hecke − *Flemish Institute for Technological Research (Vito N.V.), Mol 2400, Belgium*

Görkem Eylül Kaya − *UNAM National Nanotechnology Research Center, Bilkent University, Ankara 06800, Turkey*

Bilge Baytekin − *UNAM National Nanotechnology Research Center, Bilkent University, Ankara 06800, Turkey; Department of Chemistry, Bilkent University, Ankara 06800, Turkey;* orcid.org/0000-0002-3867-3863

https://doi.org/10.1021/acs.biomac.3c00275
Biomacromolecules 2023, 24, 3498−3509

Richard Vendamme − *Flemish Institute for Technological Research (Vito N.V.), Mol 2400, Belgium;* orcid.org/0000-0002-8931-0851

Complete contact information is available at: https://pubs.acs.org/10.1021/acs.biomac.3c00275

Notes

The authors declare no competing financial interest.

■ ACKNOWLEDGMENTS

The authors would like to thank M. de Baat and S.C. Gándara for the DPPH assays and acknowledge COST Action CA17128 "Establishment of a Pan-European Network on the Sustainable Valorisation of Lignin (LignoCOST)". VITO would like to acknowledge the province of Noord-Brabant (The Netherlands) for the financial support in the framework of the activities at the Shared Research Center Biorizon. The authors gratefully acknowledge the funding by the European Union NextGenerationEU through the Catalisti project Delicare (HBC.2022.0555).

■ REFERENCES

(1) Gamble, A. Ullmann's Encyclopedia of Industrial Chemistry. *Charlest. Advis.* **2019**, *20*, 46−50.

(2) Jedrzejczyk, M. A.; Van den Bosch, S.; Van Aelst, J.; Van Aelst, K.; Kouris, P. D.; Moalin, M.; Haenen, G. R. M. M.; Boot, M. D.; Hensen, E. J. M.; Lagrain, B.; et al. Lignin-Based Additives for Improved Thermo-Oxidative Stability of Biolubricants. *ACS Sustainable Chem. Eng.* **2021**, *9*, 12548−12559.

(3) Pisoschi, A. M.; Negulescu, G. P. Methods for total antioxidant activity determination: a review. *Biochem. Anal. Biochem.* **2011**, *1*, No. 106.

(4) (a) Neha, K.; Haider, M. R.; Pathak, A.; Yar, M. S. Medicinal prospects of antioxidants: A review. *Eur. J. Med. Chem.* **2019**, *178*, 687−704. (b) Boulebd, H. Comparative study of the radical scavenging behavior of ascorbic acid, BHT, BHA and Trolox: Experimental and theoretical study. *J. Mol. Struct.* **2020**, *1201*, No. 127210.

(5) Shahidi, F. Antioxidants in food and food antioxidants. *Nahrung/Food* **2000**, *44*, 158−163.

(6) Mahmood, Z.; Yameen, M.; Jahangeer, M.; Riaz, M.; Ghaffar, A.; Javid, I.Lignin as Natural Antioxidant Capacity. In *Lignin - Trends and Applications*; IntechOpen, 2018; Vol. *10*, pp 181−205.

(7) Özel, M.; Demir, F.; Aikebaier, A.; Kwiczak-Yiğitbaşı, J.; Baytekin, H. T.; Baytekin, B. Why Does Wood Not Get Contact Charged? Lignin as an Antistatic Additive for Common Polymers. *Chem. Mater.* **2020**, *32*, 7438−7444.

(8) Bajwa, D. S.; Pourhashem, G.; Ullah, A. H.; Bajwa, S. G. A concise review of current lignin production, applications, products and their environmental impact. *Ind. Crops Prod.* **2019**, *139*, No. 111526.

(9) (a) Dessbesell, L.; Paleologou, M.; Leitch, M.; Pulkki, R.; Xu, C. Global lignin supply overview and kraft lignin potential as an alternative for petroleum-based polymers. *Renewable Sustainable Energy Rev.* **2020**, *123*, No. 109768. (b) Glasser, W. G. About Making Lignin Great Again—Some Lessons From the Past. *Front. Chem.* **2019**, *7*, No. 565. (c) Lora, J. H.; Glasser, W. G. Recent Industrial Applications of Lignin: A Sustainable Alternative to Nonrenewable Materials. *J. Polym. Environ.* **2002**, *10*, 39−48. (d) Sadeghifar, H.; Ragauskas, A. Perspective on Technical Lignin Fractionation. *ACS Sustainable Chem. Eng.* **2020**, *8*, 8086−8101.

(10) (a) Bourbiaux, D.; Pu, J.; Rataboul, F.; Djakovitch, L.; Geantet, C.; Laurenti, D. Reductive or oxidative catalytic lignin depolymerization: An overview of recent advances. *Catal. Today* **2021**, *373*, 24−37. (b) Sun, Z.; Fridrich, B.; De Santi, A.; Elangovan, S.; Barta, K. Bright side of lignin depolymerization: toward new platform chemicals. *Chem. Rev.* **2018**, *118*, 614−678. (c) Chio, C.; Sain, M.; Qin, W. Lignin utilization: a review of lignin depolymerization from various aspects. *Renewable Sustainable Energy Rev.* **2019**, *107*, 232−249.

(11) Renders, T.; Van den Bossche, G.; Vangeel, T.; Van Aelst, K.; Sels, B. Reductive catalytic fractionation: state of the art of the lignin-first biorefinery. *Curr. Opin. Biotechnol.* **2019**, *56*, 193−201.

(12) (a) Feghali, E.; van de Pas, D. J.; Torr, K. M. Toward Bio-Based Epoxy Thermoset Polymers from Depolymerized Native Lignins Produced at the Pilot Scale. *Biomacromolecules* **2020**, *21*, 1548−1559. (b) Quinsaat, J. E. Q.; Feghali, E.; van de Pas, D. J.; Vendamme, R.; Torr, K. M. Preparation of Mechanically Robust Bio-Based Polyurethane Foams Using Depolymerized Native Lignin. *ACS Appl. Polym. Mater.* **2021**, *3*, 5845−5856.

(13) (a) Thi, H. D.; Van Aelst, K.; Van den Bosch, S.; Katahira, R.; Beckham, G. T.; Sels, B. F.; Van Geem, K. M. Identification and quantification of lignin monomers and oligomers from reductive catalytic fractionation of pine wood with GC× GC−FID/MS. *Green Chem.* **2022**, *24*, 191−206. (b) Schutyser, W.; Renders, aT.; Van den Bosch, S.; Koelewijn, S.-F.; Beckham, G.; Sels, B. F. Chemicals from lignin: an interplay of lignocellulose fractionation, depolymerisation, and upgrading. *Chem. Soc. Rev.* **2018**, *47*, 852−908.

(14) (a) Domenek, S.; Louaifi, A.; Guinault, A.; Baumberger, S. Potential of lignins as antioxidant additive in active biodegradable packaging materials. *J. Polym. Environ.* **2013**, *21*, 692−701. (b) Gadioli, R.; Waldman, W. R.; De Paoli, M. A. Lignin as a green primary antioxidant for polypropylene. *J. Appl. Polym. Sci.* **2016**, *133*, No. 43558. (c) Pouteau, C.; Dole, P.; Cathala, B.; Avérous, L.; Boquillon, N. Antioxidant properties of lignin in polypropylene. *Polym. Degrad. Stab.* **2003**, *81*, 9−18. (d) Košíková, B.; Demianova, V.; Kačuráková, M. Sulfur-free lignins as composites of polypropylene films. *J. Appl. Polym. Sci.* **1993**, *47*, 1065−1073.

(15) (a) Bass, G. F.; Epps, T. H. Recent Developments Towards Performance-enhancing Lignin-based Polymers. *Polym. Chem.* **2021**, *12*, 4130−4158. (b) Holmberg, A. L.; Stanzione, J. F.; Wool, R. P.; Epps, T. H. A Facile Method for Generating Designer Block Copolymers from Functionalized Lignin Model Compounds. *ACS Sustainable Chem. Eng.* **2014**, *2*, 569−573. (c) Mahajan, J. S.; O'Dea, R. M.; Norris, J. B.; Korley, L. T. J.; Epps, T. H. Aromatics from Lignocellulosic Biomass: A Platform for High-Performance Thermosets. *ACS Sustainable Chem. Eng.* **2020**, *8*, 15072−15096. (d) O'Dea, R. M.; Willie, J. A.; Epps, T. H. 100th Anniversary of Macromolecular Science Viewpoint: Polymers from Lignocellulosic Biomass. Current Challenges and Future Opportunities. *ACS Macro Lett.* **2020**, *9*, 476−493. (e) Wang, S.; Bassett, A. W.; Wieber, G. V.; Stanzione, J. F., III; Epps, T. H., III Effect of methoxy substituent position on thermal properties and solvent resistance of lignin-inspired poly (dimethoxyphenyl methacrylate) s. *ACS Macro Lett.* **2017**, *6*, 802−807.

(16) Bassett, A. W.; Sweet, K. R.; O'Dea, R. M.; Honnig, A. E.; Breyta, C. M.; Reilly, J. H.; La Scala, J. J.; Epps, T. H.; Stanzione, J. F. Dual-functional, aromatic, epoxy-methacrylate monomers from bio-based feedstocks and their respective epoxy-functional thermoplastics. *J. Polym. Sci.* **2020**, *58*, 673−682.

(17) Holmberg, A. L.; Nguyen, N. A.; Karavolias, M. G.; Reno, K. H.; Wool, R. P.; Epps, T. H. Softwood Lignin-Based Methacrylate Polymers with Tunable Thermal and Viscoelastic Properties. *Macromolecules* **2016**, *49*, 1286−1295.

(18) Holmberg, A. L.; Reno, K. H.; Nguyen, N. A.; Wool, R. P.; Epps, T. H. Syringyl Methacrylate, a Hardwood Lignin-Based Monomer for High-Tg Polymeric Materials. *ACS Macro Lett.* **2016**, *5*, 574−578.

(19) Wang, S.; Shuai, L.; Saha, B.; Vlachos, D. G.; Epps, T. H., III From tree to tape: direct synthesis of pressure sensitive adhesives from depolymerized raw lignocellulosic biomass. *ACS Cent. Sci.* **2018**, *4*, 701−708.

(20) Qu, W.; Huang, Y.; Luo, Y.; Kalluru, S.; Cochran, E.; Forrester, M.; Bai, X. Controlled Radical Polymerization of Crude Lignin Bio-oil Containing Multihydroxyl Molecules for Methacrylate Polymers and the Potential Applications. *ACS Sustainable Chem. Eng.* **2019**, *7*, 9050−9060.

(21) (a) Pezzana, L.; Malmstrom, E.; Johansson, M.; Sangermano, M. UV-Curable Bio-Based Polymers Derived from Industrial Pulp and Paper Processes. *Polymers* **2021**, *13*, No. 1530. (b) Sutton, J. T.; Rajan, K.; Harper, D. P.; Chmely, S. C. Lignin-Containing Photoactive Resins for 3D Printing by Stereolithography. *ACS Appl. Mater. Interfaces* **2018**, *10*, 36456−36463. (c) Voet, V. S. D.; Strating, T.; Schnelting, G. H. M.; Dijkstra, P.; Tietema, M.; Xu, J.; Woortman, A. J. J.; Loos, K.; Jager, J.; Folkersma, R. Biobased Acrylate Photocurable Resin Formulation for Stereolithography 3D Printing. *ACS Omega* **2018**, *3*, 1403−1408.
(22) Llevot, A.; Grau, E.; Carlotti, S.; Grelier, S.; Cramail, H. From lignin-derived aromatic compounds to novel biobased polymers. *Macromol. Rapid Commun.* **2016**, *37*, 9−28.
(23) (a) Tang, S. L. Y.; Smith, R. L.; Poliakoff, M. Principles of green chemistry: PRODUCTIVELY. *Green Chem.* **2005**, *7*, 761−762. (b) Zimmerman, J. B.; Anastas, P. T.; Erythropel, H. C.; Leitner, W. Designing for a green chemistry future. *Science* **2020**, *367*, 397−400.
(24) (a) de Souza, E. C.; Romero-Ortega, M.; Olivo, H. F. Lipase-mediated selective acetylation of primary alcohols in ethyl acetate. *Tetrahedron Lett.* **2018**, *59*, 287−290. (b) Heeres, A.; Vanbroekhoven, K.; Van Hecke, W. Solvent-free lipase-catalyzed production of (meth) acrylate monomers: Experimental results and kinetic modeling. *Biochem. Eng. J.* **2019**, *142*, 162−169.
(25) Ortiz, C.; Ferreira, M. L.; Barbosa, O.; dos Santos, J. C.; Rodrigues, R. C.; Berenguer-Murcia, Á.; Briand, L. E.; Fernandez-Lafuente, R. Novozym 435: the "perfect" lipase immobilized biocatalyst? *Catal. Sci. Technol.* **2019**, *9*, 2380−2420.
(26) Takeshima, H.; Satoh, K.; Kamigaito, M. Bio-based vinylphenol family: Synthesis via decarboxylation of naturally occurring cinnamic acids and living radical polymerization for functionalized polystyrenes. *J. Polym. Sci.* **2020**, *58*, 91−100.
(27) Levy, L. B. Inhibition of acrylic acid polymerization by phenothiazine and p-methoxyphenol. *J. Polym. Sci., Polym. Chem. Ed.* **1985**, *23*, 1505−1515.
(28) Idowu, L. A.; Hutchinson, R. A. Solvent effects on radical copolymerization kinetics of 2-hydroxyethyl methacrylate and butyl methacrylate. *Polymers* **2019**, *11*, No. 487.
(29) Mishra, K.; Ojha, H.; Chaudhury, N. K. Estimation of antiradical properties of antioxidants using DPPH assay: A critical review and results. *Food Chem.* **2012**, *130*, 1036−1043.
(30) Pepper, J. M.; Sundaram, G.; Dyson, G. Lignin and related compounds. III. An improved synthesis of 3-(4-hydroxy-3-methoxyphenyl)-1-propanol and 3-(4-hydroxy-3, 5-dimethoxyphenyl)-1-propanol. *Can. J. Chem.* **1971**, *49*, 3394−3395.
(31) Fineman, M.; Ross, S. D. Linear method for determining monomer reactivity ratios in copolymerization. *J. Polym. Sci.* **1950**, *5*, 259−262.
(32) Kelen, T.; TÜods, F. Analysis of the Linear Methods for Determining Copolymerization Reactivity Ratios. I. A New Improved Linear Graphic Method. *J. Macromol. Sci., Part A - Chem.* **1975**, *9*, 1−27.
(33) Mayo, F. R.; Lewis, F. M. Copolymerization. I. A Basis for Comparing the Behavior of Monomers in Copolymerization; The Copolymerization of Styrene and Methyl Methacrylate. *J. Am. Chem. Soc.* **1944**, *66*, 1594−1601.
(34) Abu-Omar, M. M.; Barta, K.; Beckham, G. T.; Luterbacher, J. S.; Ralph, J.; Rinaldi, R.; Román-Leshkov, Y.; Samec, J. S. M.; Sels, B. F.; Wang, F. Guidelines for performing lignin-first biorefining. *Energy Environ. Sci.* **2021**, *14*, 262−292.
(35) Raman, A.; Sankar, A.; Abhirami, S.; Anilkumar, A.; Saritha, A. Insights into the sustainable development of lignin-based textiles for functional applications. *Macromol. Mater. Eng.* **2022**, *307*, No. 2200114.
(36) Perrier, S. 50th Anniversary Perspective: RAFT Polymerization—A User Guide. *Macromolecules* **2017**, *50*, 7433−7447.
(37) (a) Caldwell, R. G.; Ihrig, J. L. The reactivity of phenols toward peroxy radicals. I. Inhibition of the oxidation and polymerization of methyl methacrylate by phenols in the presence of air. *J. Am. Chem. Soc.* **1962**, *84*, 2878−2886. (b) Samal, R. K.; Sahoo, P. K.; Bhattacharjee, S. P.; Samantaray, H. S. Kinetics of inhibition and retardation of methyl methacrylate polymerization by phenols. *J. Macromol. Sci., Part A - Chem.* **1986**, *23*, 203−220.
(38) Cutié, S. S.; Henton, D. E.; Powell, C.; Reim, R. E.; Smith, P. B.; Staples, T. L. The effects of MEHQ on the polymerization of acrylic acid in the preparation of superabsorbent gels. *J. Appl. Polym. Sci.* **1997**, *64*, 577−589.
(39) (a) Barclay, L. R. C.; Xi, F.; Norris, J. Q. Antioxidant properties of phenolic lignin model compounds. *J. Wood Chem. Technol.* **1997**, *17*, 73−90. (b) Ponomarenko, J.; Lauberts, M.; Dizhbite, T.; Lauberte, L.; Jurkjane, V.; Telysheva, G. Antioxidant activity of various lignins and lignin-related phenylpropanoid units with high and low molecular weight. *Holzforschung* **2015**, *69*, 795−805.
(40) (a) Yu, R.; Mandlekar, S.; Kong, A.-N. T. Molecular mechanisms of butylated hydroxylanisole-induced toxicity: Induction of apoptosis through direct release of cytochromec. *Mol. Pharmacol.* **2000**, *58*, 431−437. (b) Kim, D.-O.; Lee, C. Y. Comprehensive study on vitamin C equivalent antioxidant capacity (VCEAC) of various polyphenolics in scavenging a free radical and its structural relationship. *Crit. Rev. Food Sci. Nutr.* **2004**, *44*, 253−273.
(41) Baytekin, H. T.; Baytekin, B.; Hermans, T. M.; Kowalczyk, B.; Grzybowski, B. A. Control of Surface Charges by Radicals as a Principle of Antistatic Polymers Protecting Electronic Circuitry. *Science* **2013**, *341*, 1368−1371.
(42) Oyama, I. C.; Souza, G. P. M.; Rezende, M. C.; Montagna, L. S.; Passador, F. R. A new eco-friendly green composite for antistatic packaging: Green low-density polyethylene/glassy carbon. *Polym. Compos.* **2020**, *41*, 2744−2752.

https://doi.org/10.1021/acs.biomac.3c00275
Biomacromolecules 2023, 24, 3498−3509